IL NUOVO CIMENTO **38 C** (2015) 138
DOI 10.1393/ncc/i2015-15138-6

Colloquia: LaThuile15

# Measurement of *CP* violation in $\mathrm{B} \to \mathrm{J}/\psi \mathrm{K}^0_\mathrm{S}$ decays at LHCb

F. Meier on behalf of the LHCb Collaboration
*Fakultät Physik, Technische Universität Dortmund - Dortmund, Germany*

received 2 October 2015

**Summary.** — Analysing a data sample corresponding to an integrated luminosity of $3\,\mathrm{fb}^{-1}$ of $pp$ collisions collected by the LHCb detector at the LHC *CP* violation in $\mathrm{B}^0 \to \mathrm{J}/\psi \mathrm{K}^0_\mathrm{S}$ and $\mathrm{B}^0_\mathrm{s} \to \mathrm{J}/\psi \mathrm{K}^0_\mathrm{S}$ is measured. The results $S(\mathrm{B}^0 \to \mathrm{J}/\psi \mathrm{K}^0_\mathrm{S}) = 0.731 \pm 0.035\,(\mathrm{stat}) \pm 0.020\,(\mathrm{syst})$, $C(\mathrm{B}^0 \to \mathrm{J}/\psi \mathrm{K}^0_\mathrm{S}) = -0.038 \pm 0.032\,(\mathrm{stat}) \pm 0.005\,(\mathrm{syst})$ are consistent with the current world averages and with the Standard Model expectations. In $\mathrm{B}^0_\mathrm{s} \to \mathrm{J}/\psi \mathrm{K}^0_\mathrm{S}$ the results $A_{\Delta\Gamma}(\mathrm{B}^0_\mathrm{s} \to \mathrm{J}/\psi \mathrm{K}^0_\mathrm{S}) = 0.49 \pm {}^{0.77}_{0.65}\,(\mathrm{stat}) \pm 0.06\,(\mathrm{syst})$, $S(\mathrm{B}^0_\mathrm{s} \to \mathrm{J}/\psi \mathrm{K}^0_\mathrm{S}) = -0.08 \pm 0.40\,(\mathrm{stat}) \pm 0.08\,(\mathrm{syst})$, $C(\mathrm{B}^0_\mathrm{s} \to \mathrm{J}/\psi \mathrm{K}^0_\mathrm{S}) = -0.28 \pm 0.41\,(\mathrm{stat}) \pm 0.08\,(\mathrm{syst})$ reflect the first determination of these *CP* observables paving a new way towards the control of penguin pollutions in the determination of $\sin 2\beta$.

## 1. – Introduction

In spite of many decades of experimental scrutiny, the Standard Model of particle physics (SM) has proven to be a very successful theory. It describes the elementary particles and anti-particles as well as the fundamental forces which determine their interactions. Various predictions of the SM could be verified, *e.g.* the Higgs boson has been discovered [1,2] concluding the experimental confirmation of all fundamental particles predicted by the SM. Though, the observable matter–anti-matter asymmetry in the universe can not be explained by the SM right now. An access towards its understanding might be the study of *CP* violation which describes an asymmetry between processes under a conjugation of charge and parity. In the SM, *CP* violation is merely described by a single irreducible phase in the quark mixing sector. The unitary CKM matrix (named after N. Cabibbo, M. Kobayashi and T. Maskawa) transforms the quark eigenstates of the weak force to the mass eigenstates. The unitary conditions which sum up to zero like

$$V_{\mathrm{ud}} V^*_{\mathrm{ub}} + V_{\mathrm{cd}} V^*_{\mathrm{cb}} + V_{\mathrm{td}} V^*_{\mathrm{tb}} = 0 \tag{1}$$

can be interpreted as triangles in the complex plane whose area are a measure for the amount of *CP* violation. The parameters $V_{xy}$ are the matrix elements determining quark

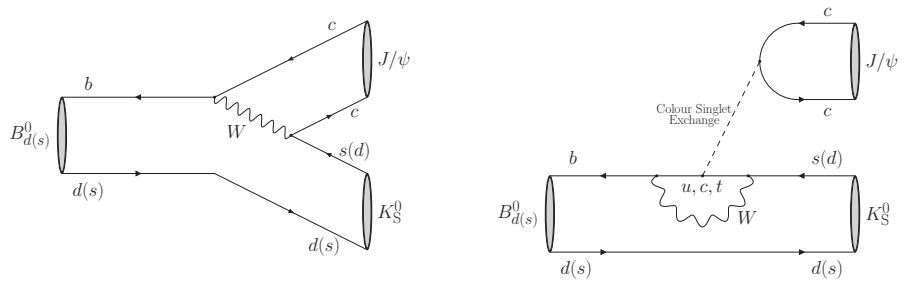


(a) Tree diagram. (b) Loop diagram.

Fig. 1. – Feynman diagrams of $\mathrm{B} \to \mathrm{J}/\psi\,\mathrm{K}^0_\mathrm{S}$ decays.

transitions of the type $x \to y$. The angle $\beta$ of one of these triangles can be defined as $\beta \equiv \arg[-(V_{\mathrm{cd}}V^*_{\mathrm{cb}})/(V_{\mathrm{td}}V^*_{\mathrm{tb}})]$. It is one of the most precisely known *CP* violation observables with a current world average of $\sin 2\beta = 0.682 \pm 0.019$ [3]. This precision is dominated by the measurements of BaBar [4] and Belle [5]. LHCb has also performed a measurement of $\sin 2\beta$ using $\mathrm{B}^0 \to \mathrm{J}/\psi\,\mathrm{K}^0_\mathrm{S}$ decays based on the first third of the currently available data sample [6], but the achieved precision is not yet competitive. This measurement is now updated with the full Run I data sample corresponding to an integrated luminosity of $3\,\mathrm{fb}^{-1}$ of *pp* collisions. In addition, a measurement of *CP* violation in the decay of $\mathrm{B}^0_\mathrm{s}$ mesons to $\mathrm{J}/\psi\,\mathrm{K}^0_\mathrm{S}$ is performed for the first time. In both analyses the final states are studied in the decay modes $\mathrm{J}/\psi \to \mu^+\mu^-$ and $\mathrm{K}^0_\mathrm{S} \to \pi^+\pi^-$.

## 2. – Time-dependent *CP* asymmetry

The time evolution of the neutral $B$ meson system can be described best in the system of mass eigenstates which differ in their mean masses ($\Delta m$) and in case of the $\mathrm{B}^0_\mathrm{s}$ mesons also in their lifetimes ($\Delta\Gamma$). This superposition evokes the possibility of oscillations between the two flavour eigenstates. As $\mathrm{J}/\psi\,\mathrm{K}^0_\mathrm{S}$ is accessible to both flavour eigenstates *CP* violation can occur in the interference between direct decay and decay after mixing. The *CP* violation can be expressed via the time-dependent asymmetry

$$\mathcal{A}(t) \equiv \frac{\Gamma(\overline{\mathrm{B}}(t) \to J/\psi \mathrm{K}^0_\mathrm{S}) - \Gamma(\mathrm{B}(t) \to J/\psi \mathrm{K}^0_\mathrm{S})}{\Gamma(\overline{\mathrm{B}}(t) \to J/\psi \mathrm{K}^0_\mathrm{S}) + \Gamma(\mathrm{B}(t) \to J/\psi \mathrm{K}^0_\mathrm{S})} = \frac{S\sin(\Delta m\, t) - C\cos(\Delta m\, t)}{\cosh(\Delta\Gamma\, t/2) + A_{\Delta\Gamma}\sinh(\Delta\Gamma\, t/2)}. \tag{2}$$

Three *CP* observables constitute the asymmetry: $S$ which describes the mixing-induced contribution, $C$ which represents the effect of direct *CP* violation and $A_{\Delta\Gamma}$. At the current level of precision the lifetime difference in the $\mathrm{B}^0$ system is compatible with zero [3]. In the analysis, it is usually fixed to zero and only the first two *CP* observables are floating.

The decay $\mathrm{B}^0 \to \mathrm{J}/\psi\,\mathrm{K}^0_\mathrm{S}$ is dominated by a $\overline{\mathrm{b}} \to \mathrm{c}\overline{\mathrm{c}}\,\mathrm{s}$ transition which can be described via a tree diagram as shown in fig. 1(a). Feynman diagrams involving loop topologies are suppressed. Their contributions are negligible at the current level of experimental precision as well as direct *CP* violation in the decay leading to $C \approx 0$ and $S \approx \sin 2\beta$.

Related through U-spin symmetry the decay $B^0_s \to J/\psi K^0_S$ can be described with a very similar Feynman diagram exchanging d-quarks with s-quarks and vice versa. With these changes the loop diagram (see fig. 1(b)) is not suppressed any more, hereby giving access to possible higher-order contributions.

## 3. – LHCb detector

The LHCb detector [7, 8] is a single-arm forward spectrometer covering the pseudo-rapidity range $2 < \eta < 5$, designed for the study of particles containing b- or c-quarks. The detector includes a high-precision tracking system consisting of a silicon-strip vertex detector surrounding the *pp* interaction region, a large-area silicon-strip detector located upstream of a dipole magnet, and three stations of silicon-strip detectors and straw drift tubes placed downstream of the magnet. The excellent vertex and tracking system results in a decay time resolution of $\sim$45 fs, a momentum resolution of $\Delta p/p = 0.4$–$0.6\%$ and an impact resolution of $\sim 20\,\mu$m. Depending on the detector response two different type of $K^0_S \to \pi^+\pi^-$ decays are considered: the first involving $K^0_S$ mesons that decay early enough for the daughter pions to be reconstructed in the vertex detector; and the second consisting of $K^0_S$ candidates that decay later such that track segments of the pions cannot be formed in the vertex detector. These categories are referred to as *long* and *downstream*, respectively. The long category has better mass, momentum and vertex resolution than the downstream category.

Different types of charged hadrons are distinguished using information from two ring-imaging Cherenkov detectors. Photon, electron, and hadron candidates are identified by a calorimeter system consisting of scintillating-pad and preshower detectors, an electromagnetic calorimeter, and a hadronic calorimeter. Muons are identified by a system composed of alternating layers of iron and multiwire proportional chambers. The online event selection system (trigger) [9] consists of a hardware stage, based on information from the calorimeter and muon systems, followed by a software stage.

## 4. – Flavour tagging

For time-dependent tagged analyses of *CP* violation it is essential to have information on the initial flavour of each reconstructed candidate. For this purpose two different types of algorithms are used at LHCb. The opposite-side (OS) tagging algorithms exploit the fact that in the *pp* collisions the b-quarks are predominantly produced in $b\bar{b}$-pairs. Therefore, the production flavour can be inferred from a study of the b-quark which is not involved in the signal decay. In the decay chain of the opposite-side b-quark particles like kaons, muons or electrons, can be produced whose charge determine the flavour of the b-quark. While these algorithms can be used for both $B^0$ and $B^0_s$ mesons the second type of tagging algorithms, referred to as same-side (SS) taggers, are specific for the two B meson types as they make use of the spectator quark which is a d-quark or an s-quark, respectively. Combined with a u-quark pions or kaons are produced whose charge again determines the b-quark flavour.

There are three quantities that indicate the performance of the flavour tagging: The tagging efficiency $\varepsilon_{\text{tag}}$ states how often the tagging algorithms have been able to deduce a tagging decision. At LHCb it is in the order of 30–40%. The mistag probability $\omega$ is the probability of a tag decision to be wrong. An estimate on this value is given by neural nets analysing the topology of the event. The tagging power $\varepsilon_{\text{eff}} = \varepsilon_{\text{tag}}(1-2\omega)^2 = \varepsilon_{\text{tag}} D^2$ gives the fraction of perfectly tagged events which would have the same statistical

power as the existing data sample. In case of the two $B \to J/\psi K^0_S$ analyses the tagging power is between 3 and 4%.

The output of the neural nets predicting the mistag probability have to be calibrated using flavour-specific decay channels, *i.e.* decay modes where the flavour at decay can definitely be determined by the charge of the decay products of the signal decay. Typically, a linear calibration is applied taking mistag asymmetries between the two flavours into account as well. For the OS tagging calibration especially $B^+ \to J/\psi K^+$ decays are used, for the SS$\pi$ calibration $B \to J/\psi K^{*0}$ decays and for the SS$K$ calibration $B^0_s \to D^+_s \pi^-$ decays.

## 5. – Measurement of *CP* violation in $B^0 \to J/\psi K^0_S$ decays [10]

Compared to the previous LHCb analysis of *CP* violation in $B^0 \to J/\psi K^0_S$ decays [6] some major improvements in the analysis strategy are achieved. Especially by including the SS$\pi$ tagger the tagging power is increased from $(2.38 \pm 0.07\%)$ to $(3.02 \pm 0.05\%)$. Using additional trigger criterions increases the signal efficiency by about 14 percentage points. Another large effect arises from optimising the selection strategy rather on a high signal efficiency than on a strong background rejection. In the cut-based selection each cut is required to have a signal efficiency of at least 99%. Cuts are applied on kinematic observables like the momentum and transverse momentum of the pions and muons or the invariant mass of the $\pi^+\pi^-$ and $\mu^+\mu^-$ system. The decay vertices of $J/\psi$ and $K^0_S$ have to be well separated from any PV and fulfil some fit quality. To eliminate $\Lambda^0_b \to J/\psi \Lambda$ background contributions the particle identification requirement on the pions is tightened if the invariant mass under a $p\pi^-$ $(\pi^+\overline{p})$ mass hypothesis is compatible with the $\Lambda$ mass. The rather long flight distance of the $K^0_S$ is exploited cutting on the decay time significance, *i.e.* the decay time of the $K^0_S$ divided by its fit uncertainty. Almost all cut values are different for long and downstream candidates.

In total, 41560 $\pm$ 270 tagged signal candidates can be used for the time-dependent analysis.

In an unbinned maximum-likelihood fit the best fit values for the 83 floating parameters of a seven dimensional probability density function (PDF) describing the distributions of the invariant mass, the decay time, the decay time error, the OS and SS$\pi$ tags and mistags are determined. This simultaneous fit is split in 24 disjoint categories being the two centre-of-mass energies (7 and 8 TeV), the $K^0_S$ type (long and downstream), two trigger configurations, and the three flavour tagging categories (exclusively tagged by OS or SS$\pi$ and tagged by both). The mass difference $\Delta m_d$, the flavour tagging calibration parameters and the production asymmetry are constrained in the fit. The value for the latter is taken from ref. [11] and adapted to the momentum and pseudorapidity distributions given in the data sample. It is also accounted for the difference between a centre-of-mass energy of $\sqrt{s} = 7$ and 8 TeV. In the end, a correction on the fit results for $S$ and $C$ is applied to account for *CP* violation in the $K^0$-$\overline{K}^0$ mixing and for the difference in the nuclear cross-sections in material between $K^0$ and $\overline{K}^0$ states [12, 13].

To evaluate the systematic uncertainties on the *CP* observables $S$ and $C$ various studies with pseudoexperiments are performed. Modifying the PDF in the simulation of the pseudoexperiments with the possible systematic effect under study and fitting with the nominal setup reveals several significant sources of systematic uncertainties. The largest uncertainty on $S$ of $\pm 0.0179$ arises from a potential tagging asymmetry in the background distribution. On $C$ the systematic uncertainty on the value for $\Delta m_d$ introduces the largest uncertainty with $\pm 0.0034$. Systematic uncertainties on the flavour

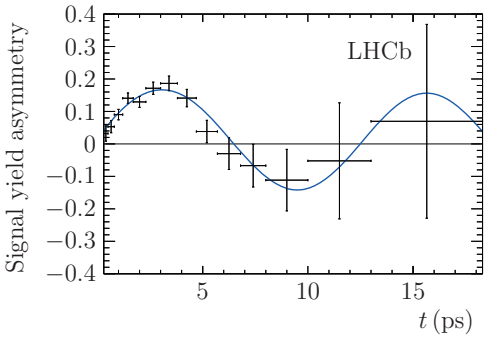


Fig. 2. – Time-dependent signal-yield asymmetry $(N_{\overline{\mathrm{B}}^0} - N_{\mathrm{B}^0})/(N_{\overline{\mathrm{B}}^0} + N_{\mathrm{B}^0})$. Here, $N_{\mathrm{B}^0}$ ($N_{\overline{\mathrm{B}}^0}$) is the number of $\mathrm{B}^0 \to \mathrm{J}/\psi\mathrm{K}^0_S$ decays with a $\mathrm{B}^0$ ($\overline{\mathrm{B}}^0$) flavour tag. The data points are obtained with the *sPlot* technique [14], assigning signal weights to the events based on a fit to the reconstructed mass distribution. The solid curve is the projection of the signal PDF.

tagging calibration parameters are responsible for the second largest systematic uncertainties both on $S$ ($\pm 0.0062$) and on $C$ ($\pm 0.0024$). Further systematic uncertainties are found to originate from the uncertainty on the length scale of the vertex detector and the assumption of $\Delta\Gamma_\mathrm{d} = 0$ which is tested by generating pseudoexperiments with its current uncertainty of $\pm 0.007\,\mathrm{ps}^{-1}$ [3]. The total systematic uncertainties are calculated by summing up the single uncertainties in quadrature resulting in $\pm 0.020$ for $S$ and $\pm 0.005$ for $C$.

In conclusion, the *CP* observables are measured to be

$$\begin{aligned} S &= \quad 0.731 \pm 0.035\,(\mathrm{stat}) \pm 0.020\,(\mathrm{syst}), \\ C &= -0.038 \pm 0.032\,(\mathrm{stat}) \pm 0.005\,(\mathrm{syst}), \end{aligned}$$

with a statistical correlation coefficient $\rho(S, C) = 0.483$. For the purpose of illustrating the fit results the time-dependent signal-yield asymmetry is given in fig. 2.

This result is in good agreement with the previous measurements by the BaBar and Belle collaborations [4, 5] while providing a similar precision.

## 6. – Measurement of the time-dependent CP asymmetries in $\mathrm{B}^0_\mathrm{s} \to \mathrm{J}/\psi\mathrm{K}^0_\mathrm{s}$ [15]

Due to the 25 times lower branching fraction and the four times lower production fraction in $pp$ collisions there are 100 times fewer $\mathrm{B}^0_\mathrm{s}$ than $\mathrm{B}^0$ candidates. LHCb's mass resolution does not allow for a complete separation of the two. Therefore, it is unavoidable to include $\mathrm{B}^0 \to \mathrm{J}/\psi\mathrm{K}^0_\mathrm{s}$ decays when studying $\mathrm{B}^0_\mathrm{s} \to \mathrm{J}/\psi\mathrm{K}^0_\mathrm{s}$ decays and the $\mathrm{J}/\psi\mathrm{K}^0_\mathrm{s}$ mass range is analysed from 5180–5520 $\mathrm{MeV}/\mathrm{c}^2$ (see fig. 3). In the offline selection the more populated $\mathrm{B}^0$ peak is used as the signal template as the kinematic difference to the $\mathrm{B}^0_\mathrm{s}$ decays is negligible. After an initial selection which removes obvious background candidates a two-stage neural net is implemented where the first one is made for eliminating backgrounds from $\mathrm{B} \to \mathrm{J}/\psi\mathrm{K}^*$ decays and the second for the suppression of combinatorial background.

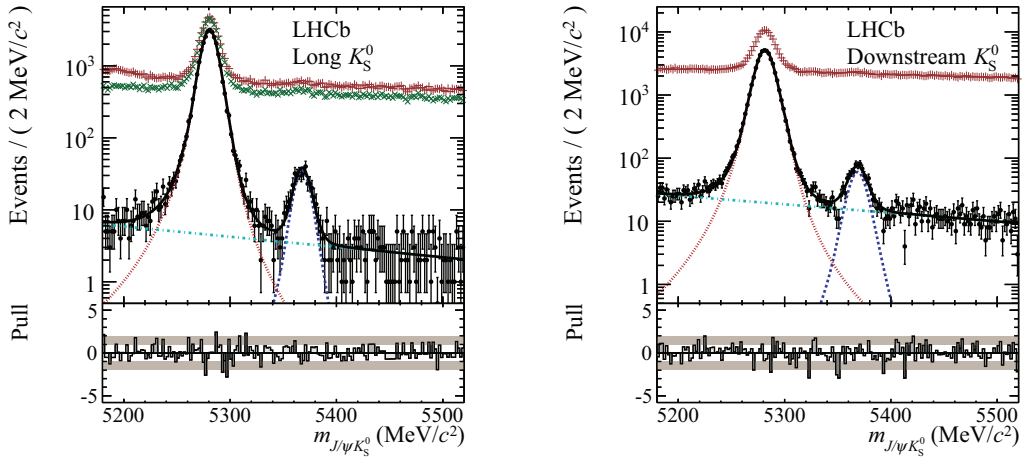


Fig. 3. – Mass distribution of B candidates at different stages of the event selection for the (left) long $K^0_S$ and (right) downstream $K^0_S$ sample. The data sample after initial selection (red, +), after the first neural net (green, ×) and after the second neural net (black, •) are shown. Overlaid are projections of the fit. The shown components are $B^0_s \to J/\psi K^0_S$ (dark blue, dashed), $B^0 \to J/\psi K^0_S$ (red, dotted) and combinatorial background (turquoise, dash-dotted).

The PDF used in the unbinned maximum likelihood fit is a sum of a $B^0$ signal component, a $B^0_s$ signal component and a combinatorial background. The long and the downstream samples are modelled separately but fitted simultaneously. The common parameters are the five *CP* observables ($A_{\Delta\Gamma}$, $S$ and $C$ of the $B^0_s$ system; $S$ and $C$ of the $B^0$ system), the lifetimes $\tau_{B^0}$ and $\tau_{B^0_s}$, and the mass and lifetime difference parameters ($\Delta m_d$, $\Delta m_s$, $\Delta\Gamma_s$) which are constrained to their world averages [3].

Significant systematic uncertainties on $A_{\Delta\Gamma}$ arise from the mass modelling, the decay-time acceptance and the decay-time resolution. The latter has also an systematic influence on $S$ and $C$, as well as the tagging calibration and the correlation between invariant mass and decay time which is neglected in the fit.

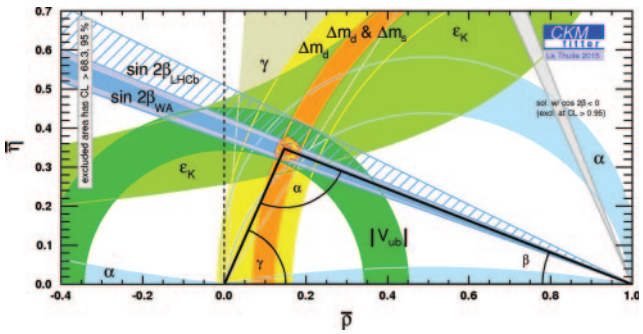


Fig. 4. – CKM triangle in the $\bar{\eta}$-$\bar{\rho}$ plane. The dark blue area shows the uncertainty band of $\sin 2\beta$ including LHCb's latest result, while the hatched area shows the LHCb measurement only.

The results of the $B^0_s \to J/\psi K^0_S$ *CP* asymmetries

$$\begin{aligned} A_{\Delta\Gamma}\left(B^0_s \to J/\psi K^0_S\right) &= \quad 0.49 \pm {}^{0.77}_{0.65}\ (\text{stat}) \pm 0.06\ (\text{syst}), \\ S\left(B^0_s \to J/\psi K^0_S\right) &= -0.08 \pm 0.40\ (\text{stat}) \pm 0.08\ (\text{syst}), \\ C\left(B^0_s \to J/\psi K^0_S\right) &= -0.28 \pm 0.41\ (\text{stat}) \pm 0.08\ (\text{syst}) \end{aligned}$$

represent the first determination of these observables.

## 7. – Conclusion

The most precise measurement of time-dependent *CP* violation at a hadron collider is achieved in the study of $B^0 \to J/\psi K^0_S$ decays. In fig. 4 the uncertainty bands for $\sin 2\beta$ of the world average and of LHCb's result are marked. It is visible that LHCb's result is in better agreement with the measurements of other quantities constraining the CKM triangle than the previous determinations of $\sin 2\beta$ by the *B*-factories. However, the statistical limitation still requires more data to validate this trend.

As most of the systematic uncertainties in the analysis of *CP* violation in $B^0 \to J/\psi K^0_S$ scale with the statistical precision further improvements in the sensitivity can be expected with the upcoming Run II of the LHCb experiment. Then, a control of penguin pollutions will become more and more relevant. A step towards this goal is achieved through the first determination of *CP* violation in $B^0_s \to J/\psi K^0_S$ decays.

REFERENCES


[1] Aad G. *et al.* (ATLAS Collaboration), *Phys. Lett. B*, **716** (2012) 1, arXiv:1207.7214.
[2] Chatrchyan S. *et al.* (CMS Collaboration), *Phys. Lett. B*, **716** (2012) 30, arXiv:1207.7235.
[3] Olive K. A. *et al.* (Particle Data Group), *Chin. Phys. C*, **38** (2014) 090001.
[4] Aubert B. *et al.* (BaBar Collaboration), *Phys. Rev. D*, **79** (2009) 072009, arXiv:0902.1708.
[5] Adachi I. *et al.* (Belle Collaboration), *Phys. Rev. Lett.*, **108** (2012) 171802, arXiv:1201.4643.
[6] Aaij R. *et al.* (LHCb Collaboration), *Phys. Lett. B*, **721** (2013) 24, arXiv:1211.6093.
[7] Alves A. A. jr. *et al.* (LHCb Collaboration), *JINST*, **3** (2008) S08005.
[8] Aaij R. *et al.* (LHCb Collaboration), *Int. J. Mod. Phys. A*, **30** (2015) 1530022, arXiv:1412.6352.
[9] Aaij R. *et al.*, *JINST*, **8** (2013) P04022, arXiv:1211.3055.
[10] Aaij R. *et al.* (LHCb Collaboration), *Phys. Rev. Lett.*, **115** (2015) 031601, arXiv:1503.07089.
[11] Aaij R. *et al.* (LHCb Collaboration), *Phys. Lett. B*, **739** (2014) 218, arXiv:1408.0275.
[12] Fetscher W. *et al.*, *Z. Phys. C*, **72** (1996) 543.
[13] Ko B. R., Won E., Golob B. and Pakhlov P., *Phys. Rev. D*, **84** (2011) 111501(R), arXiv:1006.1938.
[14] Pivk M. and Le Diberder F. R., *Nucl. Instrum. Methods A*, **555** (2005) 356, arXiv:physics/0402083.
[15] Aaij R. *et al.* (LHCb Collaboration), *JHEP*, **06** (2015) 131, arXiv:1503.07055.